Transactions, SMiRT-26
Berlin/Potsdam, Germany, July 10-15, 2022
Division XI

AUTOMATED QUALITY ASSESSMENT OF MODULAR COMPONENTS FOR CONSTRUCTION OF NUCLEAR ENERGY FACILITIES USING 3D AS-BUILT MODELS AND BIM

Guang-Yu Nie[1], and Kevin Han[2]

[1]Postdoctoral Scholar, Center for Nuclear Energy Facilities and Structures, NC State University, Raleigh, NC, USA (gnie@ncsu.edu)
[2]Assistant Professor, Center for Nuclear Energy Facilities and Structures, NC State University, Raleigh, NC, USA

ABSTRACT

Modularization has been perceived as one of the solutions for decreasing construction overnight costs and schedules. However, when modules or connecting components have quality issues and/or manufacturing and construction deviations, they often need to be repaired on-site. If modules are not repairable on-site, remanufacturing and shipping will lead to greater delays and cost overruns. This paper presents a general compatibility analysis method and a general geometric inspection method to check whether a module is compatible with its connecting components. After scanning the as-built modules made in different manufacturing plants and/or construction sites, the compatibility analysis method will check the compatibility among connecting modules automatically and remotely, and inspects the geometric defects for all modules. The proposed system is validated using a piping system for its efficiency and robustness.

Keywords: modularization, compatibility, geometric defects, inspection, pipe system.

INTRODUCTION

Modularization has been perceived as one of the solutions to reduce construction overnight costs and schedules (Hopf, 2013; MIT, 2018). It allows parts of a module or building components to be produced from off-site facilities that are controlled environments, allowing higher productivity and consistent quality (Tak et al., 2020; Mousaei et al., 2021; Pooladvand et al., 2021). Then these modules are shipped to a jobsite for assembly. However, if there is a defect identified at the jobsite, the module needs to be repaired. If not repairable (e.g., due to high quality standards required by nuclear energy facilities), it has to be remanufactured and shipped again to the jobsite, leading to additional cost overruns and delays (Hyun et al., 2020; Shahtaheri et al., 2017).

Researchers have investigated use of reality capture technologies that generate 3D point clouds of modules and comparing them against their design models (3D CAD/building information models (BIM)) which would allow identifying geometric defects at the manufacturing facility before shipment and installation (Guo et al., 2020). This kind of quality assessment method has been applied to various types of modules, such as piping spools (Safa et al., 2015), precast concrete modules (Kim et al., 2020; Wang et al., 2016), and industrial modules (Guo et al., 2020). However, they focus a single module or component based on the corresponding building information model (BIM). They can deviations against the design model but they cannot capture incompatibilities among connecting components. For example, a pipe module may not be compatible with its connecting modules due to changing site conditions, even if each module meets the required geometric standards.

To address this gap in knowledge, this paper presents a general compatibility analysis method that checks the gap between two as-built modules and inspect geometric deviations between an as-built module and its design model (CAD/BIM). This approach ensures the quality of modules that are fabricated at different locations prior to shipment, preventing potential incompatibility issues at the jobsite during assembly. A case study using a pipe system was prepared to validate the effectiveness and robustness of the presented method in checking the module-to-module compatibility and inspecting geometric deviations.

RELATED WORKS

This section summarizes existing methods relevant to the presented quality assessment methods.

Module Position Checking

Researchers are currently exploring new technologies to detect and reduce misplacement automatically. Nahangi et al. (Nahangi et al., 2014) present an automated approach for monitoring and assessing fabricated pipe spools using automated point clouds-to-BIM registration. However, this method works only on uncluttered point clouds. Wang et al. (Wang et al., 2021) propose a novel framework that integrates the latest computer vision methods to automatically monitor the construction progress of precast walls, one of the essential components in precast construction. This framework combines object detection, instance segmentation, and multiple-object tracking to collect precast walls' location and temporal information from the surveillance videos recording the construction phase. Status information identified and collected is stored in a JavaScript object notation (JSON) format and then sent into a corresponding BIM to timestamp the wall components. Each method in the framework is evaluated, respectively, and the demonstration on a real project proves the feasibility, convenience, and efficiency of this vision-based framework. Wang et al. (Wang et al. 2017) develop a technique for automated position estimation of rebars on reinforced precast concrete elements using colored laser scan data. A novel mixed pixel filter is developed to remove mixed pixels from the raw scan data based on both distance and color difference. A one-class classifier is used to extract rebars from all the data based on geometric and color features of points. Furthermore, a novel rebar recognition algorithm is developed to recognize individual rebars based on two newly defined metrics. Czerniawski et al. (Czerniawski et al. 2016) present an automated method for locating and extracting pipe spools in cluttered point cloud scans. The method is based on local data level curvature estimation, clustering, and bag-of-features matching. Nahangi et al. (Nahangi et al., 2016) present an algorithm for automated quantification of discrepancies for components of assemblies. Rather than using dense point clouds, the geometric skeleton (wireframe) of assemblies is extracted for further manipulation once the as-built status is captured using the appropriate method. The extracted skeletons, which abstractly represent the designed and built states, are registered using a constrained ICP algorithm. In order to identify the points making up each straight segment, the skeletons are clustered, and a straight line is fit to each resulting cluster. The corresponding segments in both states are then compared and investigated for quantifying the incurred discrepancy in the form of a rigid transformation.

Module Dimension Checking

In addition to checking modules position, module dimensions are another critical factor. Kim et al. (Kim et al., 2015) establish an end-to-end framework for dimensional and surface quality assessment of precast concrete elements based on BIM and 3D laser scanning, which is composed of four parts: (1) the inspection checklists; (2) the inspection procedure; (3) the selection of an optimal scanner and scan parameters; and (4) the inspection data storage and delivery method. Kim et al. (Kim et al., 2014) present a fully automated and non-contact measurement technique that measures and assesses precast concrete panels' dimensions and quality using a terrestrial laser scanner (TLS). An edge and corner extraction technique is developed to estimate the dimensional properties of precast concrete panels from TLS scanning data. To increase the measurement accuracy, a compensation model is employed to account for the dimension losses caused by

an intrinsic limitation of TLS. Alzraiee et al. (Alzraiee et al., 2020) propose an approach to ensure embeds are positioned as per the design and within the tolerance limits stated in ACI 117. The proposed approach maps the BIM model geometry into 3D point clouds of the as-built construction. The mapping process uses different computing platforms that eventually result in a position deviation report in the x, y, and z directions. Kim et al. (Kim et al., 2020) develop a laser scanning-based technique that automatically assesses the key Dimensional quality assessment (DQA) checklists of reinforced concrete (RC) elements, including rebar spacing and concrete cover with respect to the formwork. To this end, a noise removal algorithm is developed based on the known geometric configuration of formwork and rebar to remove background noise and mixed pixels. Key features of the formwork and rebar are then automatically extracted using the principal component analysis and the RANSAC. Enshassi et al. (Enshassi et al., 2020) introduce a systematic methodology that employs Bayesian inference theory for the dynamic assessment and proactive management of excessive geometric variability issues. The developed methodology includes a practical process for continual (1) updating of initial estimates of the performance of tolerance-based mitigation strategies based on real-time data, (2) reassessment of the risk profile, and (3) refinement of risk response decisions.

Figure 1. An overview of the proposed compatibility analysis framework.

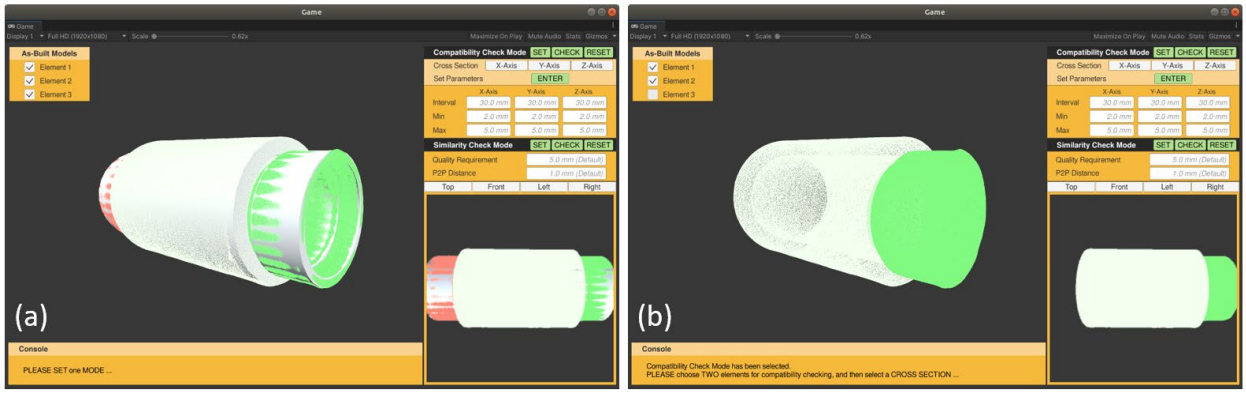

Figure 2. Construction performance monitoring system. (a) As-built modules and BIM registration. (b) Assembed modules.

METHODS

As shown in Fig. 1, the proposed compatibility analysis framework has three main steps. In the first step, we employ laser scanners to get the 3D point clouds of as-built modules from different manufacturing plants and/or construction sites. These modules need to be assembled at a jobsite. Next, we assemble the 3D point clouds of as-built modules virtually by registering 3D point clouds with the corresponding BIMs. We implement the automated compatibility assessment and geometric inspection in the final step. We utilize an example of a pipe system to show each step. As shown in Fig. 2(a), white meshes are as-planned modules (i.e., BIMs) of two joints and a pipe, and each side of the pipe connects with a joint. The green and red objects are the scanned 3D point clouds of as-built joints, and the white component is the scanned 3D point clouds of an as-built pipe. The 3D point clouds of two joints and the pipe are assembled virtually by registering them with their corresponding BIMs.

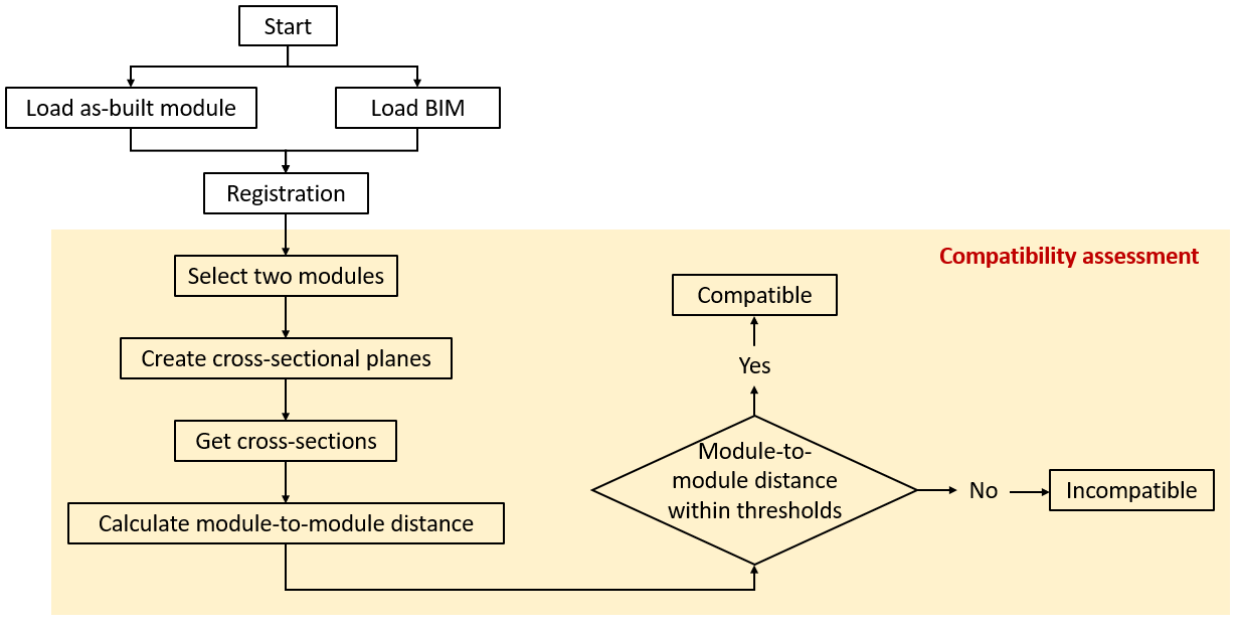

Figure 3. Flowchart of the compatibility assessment

Compatibility Assessment

Compatibility assessment checks the gap between two as-built modules to evaluate whether a module is compatible with its connecting components. This method calculates the distance between two 3D point clouds at the arbitrary cross-sections of connecting components. These two 3D point clouds are the scanned data of two as-built modules that are produced in different areas but will be assembled in the future. Fig. 3 illustrates the overall steps of the proposed compatibility analysis approach. We collect the scanning 3D point clouds of as-built modules and manually register the 3D point clouds to the corresponding BIM in our developed monitoring system. Then, we select a pair of as-built modules for further compatibility analysis. For example, Fig. 2(b) shows that the joint with green 3D point clouds and the pipe with white 3D point clouds are selected for further compatibility analysis.

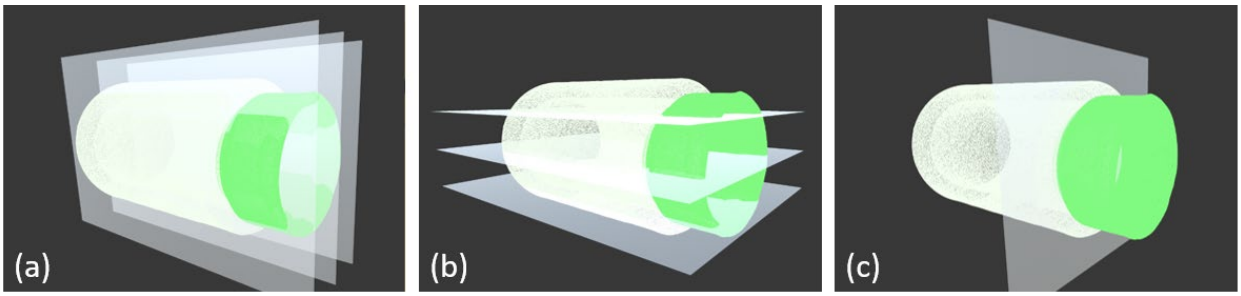

Figure 4. Multiple cross-sectional planes are created along (a) x-Axis, (b) y-Axis, (c) z-Axis directions.

In our study, the compatibility at arbitrary cross-sections of connecting components can be checked by setting the cross-sections in any direction (i.e., x-, y-, z-Axis). We select one direction from three and utilize cross-sectional planes to get the cross-sections of point clouds. Firstly, we set up the interval distance between two cross-sectional planes and create multiple cross-sectional planes along the unique direction. The white semi-transparent cross-sectional planes in Fig. 4 are created along the x-Axis (Fig. 4(a)), y-Axis (Fig. 4(b)), and z-Axis (Fig. 4(c)) direction, respectively, with an interval of 30 millimeters (mm). In Fig. 4(c), only one plane is created along the z-Axis when the interval is 30 mm. Then, we clip the 3D point

clouds to get a thin cross-section cluster associated with each cross-sectional plane. The cross-section cluster contains all points lying close to the plane within an offset value, which is defined as follows:

$$plane - offset < V_k < plane + offset, k \in \{1{:}m\} \quad (1)$$

Where V_k is a point of the 3D point clouds of an as-built module, and m is the total number of points in the 3D point clouds. *plane* is the 3D coordinate of the center of the cross-sectional plane. The 3D point within this range will be kept to generate a cross-section cluster. Fig. 8(a) shows that three cross-sections are generated associated with each plane along the x-Axis direction. Fig. 8(b) shows the cross-section associated with the front cross-sectional plane shown in Fig. 8(a), where blue thin 3D point clouds clusters are the cross-sections of the pipe, and red thin 3D point clouds clusters are the cross-sections of the joint.

After generating cross-sections, we calculate the distance between every point of the 3D point clouds of one as-built module, PC_1, and every point of the 3D point clouds of another as-built module, PC_2, to find the nearest location of two cross-sections. The minimum distance (d) can be calculated as follows:

$$d = \min\left(\left|V_{1,i} - V_{2,j}\right| : i \in \{1{:}n_1\}, j \in \{1{:}n_2\}\right) \quad (2)$$

Where $V_{1,i}$ is a 3D point with an index of i in PC_1, and $V_{2,j}$ is a 3D point with an index of j in PC_2. Also, n_1 and n_2 are the total numbers of 3D points PC_1 and PC_2, respectively. Next, the two points with minimum distance are highlighted to the user. The module-to-module compatibility at a special cross-section will be analyzed by comparing the minimum distance of the gap with the quality thresholds set up by users. If the minimum distance is in the upper and lower thresholds range, these two as-built modules are compatible at this cross-section. Otherwise, these two modules are incompatible. The upper bound threshold is the maximum tolerable gap, and the minimum threshold is the minimum tolerable gap. The lower value for the thresholds corresponds to a tighter joint, while higher values of the thresholds correspond to having more gaps between two modules. As shown in Fig. 8(b), the two nearest points are highlighted by green spheres (shown in a red dashed circle), and the location of the area with minimum distance is zoomed in and shown in the right-bottom subwindows. We set the minimum and maximum quality thresholds at 2.0mm and 5.0mm, respectively. As shown in the console window, the minimum distance between two cross-sections (i.e., the distance between two green spheres) is 3.94mm, which means that the joint and pipe are compatible at the selected cross-section.

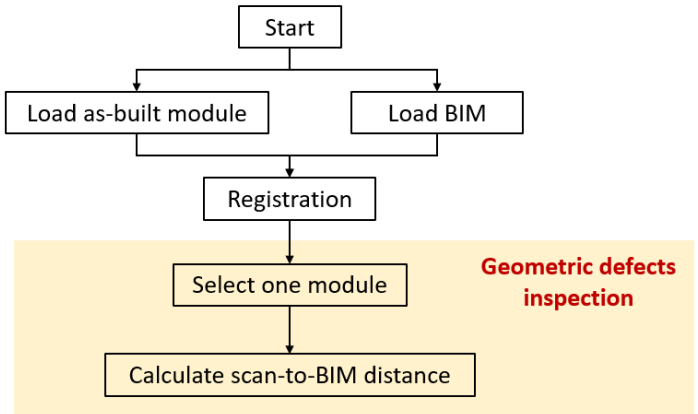

Figure 5. Flowchart of the geometric inspection.

Geometric Inspection

After implementing compatibility assessment, it is necessary to inspect the quality of each as-built module in terms of geometry. Fig. 5 illustrates the overall steps of the developed geometric inspection. We select one module for further geometric inspection. This inspection will check geometric deviations between 3D point clouds of the selected single as-built module and its corresponding BIM, implemented by following the *Algorithm 1*. We search the nearest mesh for each point of 3D point clouds, calculate the distance between point and mesh, and check whether this point is inside BIM. If the point is outside of BIM, the distance between the point and BIM is a negative value. Otherwise, the distance is a positive value.

Algorithm 1 Calculate Signed Distance Between 3D Point Clouds and BIM
Input: *Points* vector3D, *Meshes* mesh
Output: dist *list*

```
function CalculateSignedDistance(Points, Meshes)
    for Point in Points do
        min_dist = 100000
        // find closest meshes for each point
        for Mesh in Meshes do
            dist1 = Point2MeshDistance(Point, Mesh)
            if dist1 < min_dist then
                min_dist = dist1
            end if
        end for
        // check if point is inside of BIM
        if point is inside of Meshes then
            dist.append(min_dist)
        else if point is outside of Meshes then
            dist.append(- min_dist)
        end if
    end for
    return dist
end function
```

EXPERIMENTAL SETUP

This section introduces the devices and software used in our study to collect data and create the construction performance monitoring system. We employ a pipe system to verify our proposed system. As shown in Fig. 7, this pipe system consists of two joints and one pipe. Before shipment and installation, we measure the gap between each pair of pipe and joint during the inspection process and check the geometric defects of each as-built module.

Devices and Software

In this study, we employ the Unity3D software to create the construction performance monitoring system, a powerful cross-platform 3D engine developed by Unity. To achieve high-performance computing and 3D scene rendering, we employ a Dell Alienware Aurora R7 desktop with 8th Gen Intel Core i7-8700 and NVIDIA GeForce GTX 2080 graphics processing unit (GPU).

Data Collection

Figure 7 shows photos, scanned models, BIM of every module of the pipe system. To generate the as-built models of the module and its connecting part (i.e., building component), we employ an Artec Leo laser scanner to scan each module to get their 3D point clouds. Artec Leo is a hand-held scanner that can achieve an accuracy of up to 0.1 mm. The pipe was placed on the rotary table while 3D hand-held scanner stayed fixed to generate a 3D scanned model. Tab. 1 shows the details of each component, including the number of points, density of 3D point clouds, number of vertices and faces of BIM, size of as-built modules.

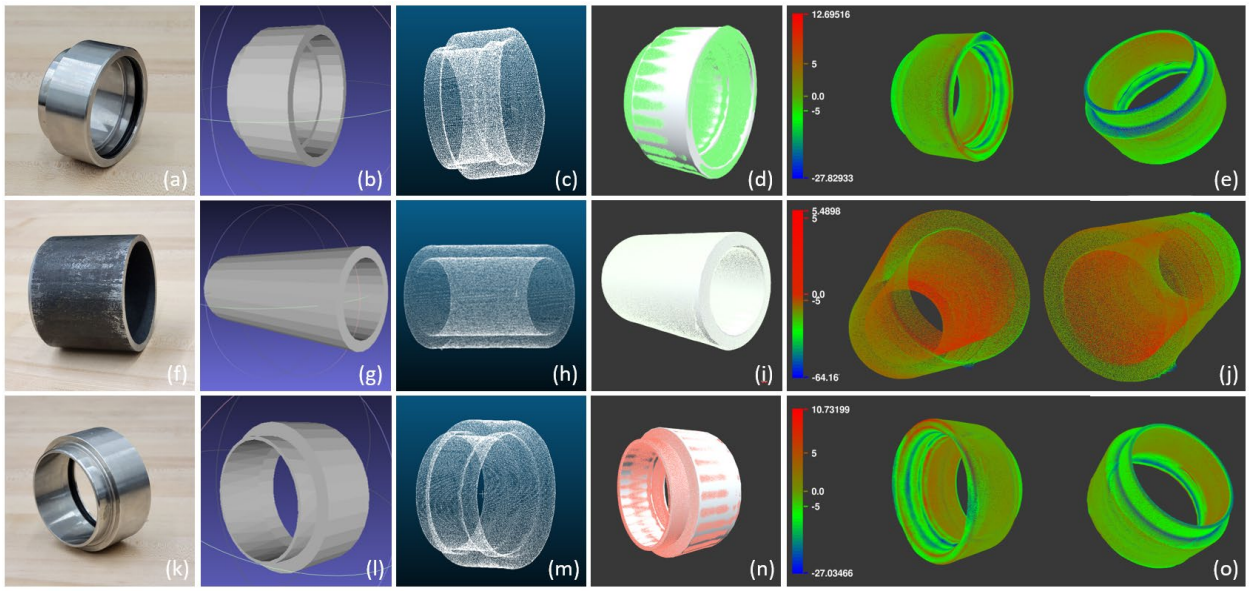

Figure 7. 1st column: photos of as-built modules; 2nd column: BIM/CAD model; 3rd column: scanned models/ 3D point clouds; 4th column: registration results between scanned model and BIM; 5th column: geometric deviations.

Table 1: Geometric size of modules in the pipe system.

	3D Point Clouds		BIM		Geometry	
	Number of Points	Density	Number of Vertices	Number of Faces	Outer Diameter	Length
Joint (Green)	999,873	38.00/mm^2	448	448	90.10mm	47.14mm
Pipe	1,000,026	5.92/mm^2	448	448	98.68mm	76.22mm
Joint(Red)	999,873	38.00/mm^2	448	448	90.10mm	47.14mm

Parameter Setting

In our experiment, there are many parameters needed to be set up. Fig. 8 (b) shows the window of our proposed system. The left-top panel is used to select the elements that are inspected, currently, there are three modules. In Fig. 2(b), we select the right joint and pipe for compatibility analysis. The right-top panel is to set up the parameters used for compatibility checking. *Interval* is used to set the interval between two neighbor planes to create cross-sectional planes; *Min* and *Max* are used to set the minimum and maximum quality thresholds to analyze the compatibility of each pair of connected components. The right-middle panel is used to set up parameters for geometric inspection. *Quality requirement* is the maximum tolerance

if the as-built module has geometric defects, which shows the maximum distance between the 3D point clouds of the as-built module and its corresponding BIM.

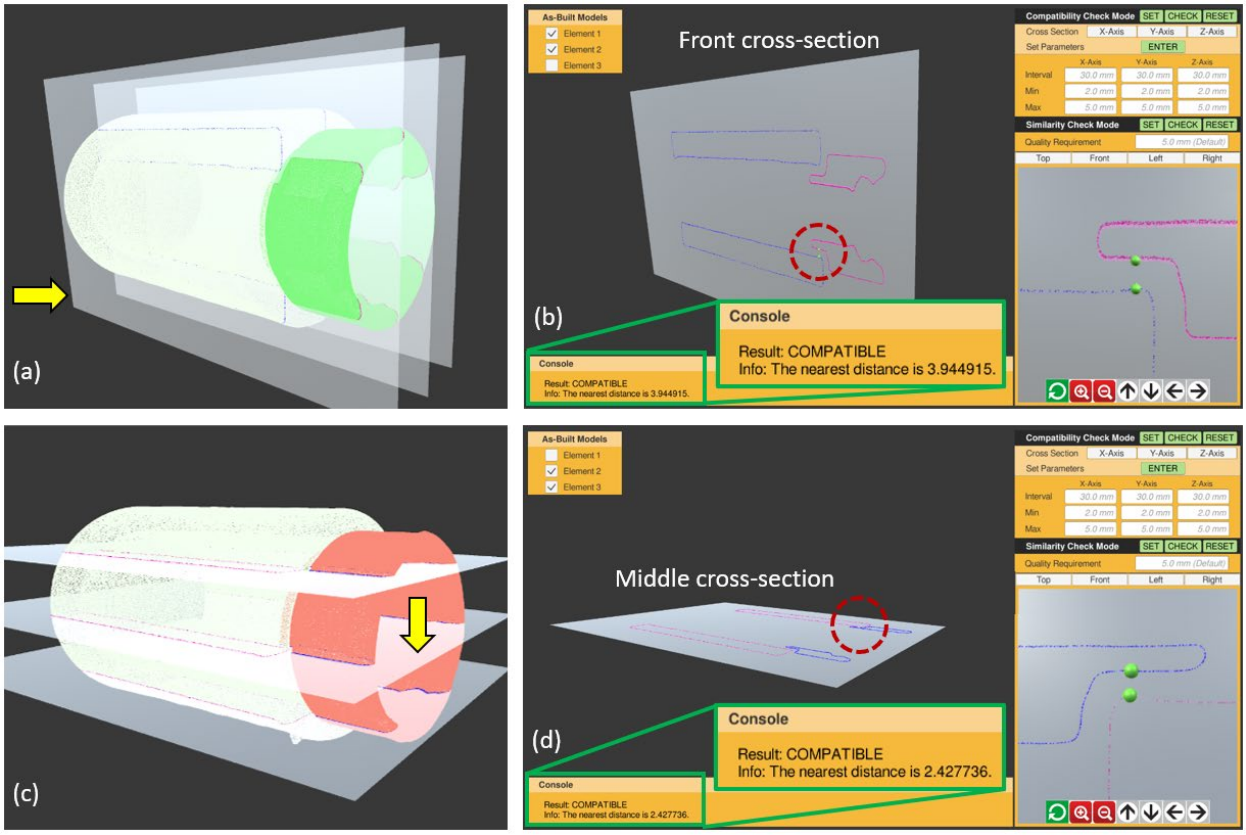

Figure 8. Results of compatibility analysis for each pair of connected componends. 1st column: Calculated cross-sections associated with cross-sectional planes. 2nd column: Results of comparibility checking.

EXPERIMENTAL RESULTS

Compatibility Analysis

Fig. 8 shows two examples when checking the compatibility between as-built pipe and each as-built joint. The figures in the first row show the compatibility analysis results between the pipe and right joint. As shown in Fig. 8(a), three cross-sectional planes are generated along the x-Axis direction, and three cross-sections are created associated with corresponding cross-sectional planes. Fig. 8(b) shows the result of compatibility checking for the cross-section at the front cross-sectional plane in Fig. 8(a). Two green spheres are generated and marked in the red circle, and the right-bottom subwindow shows the zoomed-in result. At this location, two cross-sections have a minimum distance, which means that when assembling pipe and joint, the gap between the pipe and joint is the smallest at this place. As shown in the console window, the nearest distance is 3.94 mm after assembling, which shows that the as-built pipe and joint are compatible. The figures in the second row show the compatibility analysis results between the pipe and the left joint. When implementing checking, three cross-sectional planes are generated along the y-Axis direction. We check the compatibility at the middle cross-sectional plane. As shown in Fig. 8(d), the nearest distance is 2.43 mm after assembling the pipe and left joint, which shows that the as-built pipe and as-built joint are compatible.

Geometric Inspection

Fig. 7 shows the results of geometric inspection for each component of the pipe system. As shown in Fig. 7(d), the as-built right joint is aligned to its corresponding BIM. Some parts of the joint are inside of BIM, while some parts of the joint are outside of BIM. Fig. 7(e) shows the results of the geometric deviations between the as-built right joint and its corresponding BIM from two view angles, where the blue points represent the points that are outside the BIM, and the red points represent those that are inside the BIM. For the points outside of BIM, the maximum distance between points and BIM is 27.83mm, while for the points inside of BIM, the maximum distance between points and BIM is 12.70mm. For these areas, the distances are larger than the quality thresholds. Fig. 7(j) shows the geometric deviations between the as-built pipe and its corresponding BIM. For the points outside of BIM, the maximum distance between points and BIM is 64.16mm, while for the points inside of BIM, the maximum distance between points and BIM is 5.49mm. Fig. 7(o) shows the geometric deviations between the as-built left joint and its corresponding BIM. For the points outside of BIM, the maximum distance between points and BIM is 27.03mm, while for the points inside of BIM, the maximum distance between points and BIM is 10.73mm.

As shown in Fig. 7(e), Fig. 7(j), and Fig.7(o), the blue points are distributed on the edges of the joint and pipe, and the green points are distributed on their coupling surfaces, which shows that the as-built module has severe geometric defects in its edges but has almost no defects on the coupled surfaces. Although there are severe geometric defects on the edges, these parts do not affect the connection between the pipe and each joint.

CONCLUSIONS

This paper presents a generalized method for compatibility checking of fabricated components and the geometric inspection of as-built modules. We assemble the as-built modules virtually and utilize the compatibility monitoring system to detect incompatibilities between modules and geometric defects of each component in modular construction. The system was tested and validated in a pipe system, demonstrated the effectiveness and robustness of the proposed method for compatibility analysis on the as-built elements, and verified the compatibility of the as-built models.

REFERENCES

Hopf, J. (2013). "How Can Nuclear Construction Costs Be Reduced?" ANS Nuclear Cafe, <http://ansnuclearcafe.org/2013/01/24/how-can-nuclear-construction-costs-be reduced/#sthash.qKKjD11S.eqMvNSih.dpbs> (Dec. 1, 2017).

MIT. (2018). "The Future of Nuclear Energy In A Carbon-Constrained World An Interdisciplinary MIT Study." *MIT Energy Initiative*.

Tak, A. N., Taghaddos, H., Mousaei, A., & Hermann, U. R. (2020). "Evaluating Industrial Modularization Strategies: Local vs. Overseas Fabrication." *Automation in Construction*, 114, 103175

Mousaei, A., Taghaddos, H., Nekouvaght Tak, A., Behzadipour, S., & Hermann, U. (2021). "Optimized Mobile Crane Path Planning in Discretized Polar Space." *Journal of Construction Engineering and Management*, 147(5), 04021036.

Pooladvand, S., Taghaddos, H., Eslami, A., Nekouvaght Tak, A., & Hermann, U. (2021). "Evaluating Mobile Crane Lift Operations Using an Interactive Virtual Reality System." *Journal of Construction Engineering and Management*, 147(11), 04021154.

Hyun, H., Kim, H., Lee, H. S., Park, M., and Lee, J. (2020). "Integrated Design Process for Modular Construction Projects to Reduce Rework." *Sustainability (Switzerland)*, MDPI AG, 12(2), 530.

Shahtaheri, Y., Rausch, C., West, J., Haas, C., and Nahangi, M. (2017). "Managing Risk in Modular Construction Using Dimensional and Geometric Tolerance Strategies." *Automation in Construction*, Elsevier, 83, 303–315.

Guo, J., Wang, Q., and Park, J. H. (2020). "Geometric Quality Inspection of Prefabricated MEP Modules With 3D Laser Scanning." *Automation in Construction*, Elsevier B.V., 111, 103053.

Safa, M., Shahi, A., Nahangi, M., Haas, C., and Noori, H. (2015). "Automating Measurement Process To Improve Quality Management For Piping Fabrication." *Structures*, Elsevier Ltd, 3, 71–80.

Kim, M. K., Thedja, J. P. P., and Wang, Q. (2020). "Automated Dimensional Quality Assessment for Formwork and Rebar of Reinforced Concrete Components Using 3D Point Cloud Data." *Automation in Construction*, Elsevier B.V., 112, 103077.

Wang, Q., Kim, M. K., Cheng, J. C. P., and Sohn, H. (2016). "Automated Quality Assessment of Precast Concrete Elements with Geometry Irregularities Using Terrestrial Laser Scanning." *Automation in Construction, Elsevier B.V.*, 68, 170–182.

Nahangi, M., & Haas, C. T. (2014). "Automated 3D Compliance Checking in Pipe Spool Fabrication." *Advanced Engineering Informatics*. 28(4), 360-369.

Wang, Z., Zhang, Q., Yang, B., Wu, T., Lei, K., Zhang, B., & Fang, T. (2021). "Vision-Based Framework For Automatic Progress Monitoring of Precast Walls by Using Surveillance Videos During The Construction Phase." *Journal of Computing in Civil Engineering*, 35(1), 04020056.

Wang, Q., Cheng, J. C., & Sohn, H. (2017). "Automated Estimation of Reinforced Precast Concrete Rebar Positions Using Colored Laser Scan Data." *Computer-Aided Civil and Infrastructure Engineering*, 32(9), 787-802.

Czerniawski, T., Nahangi, M., Haas, C., & Walbridge, S. (2016). "Pipe Spool Recognition in Cluttered Point Clouds Using a Curvature-Based Shape Descriptor." *Automation in Construction*, 71, 346-358.

Nahangi, M., & Haas, C. T. (2016). "Skeleton-Based Discrepancy Feedback for Automated Realignment of Industrial Assemblies." *Automation in construction*, 61, 147-161.

Kim, M. K., Cheng, J. C., Sohn, H., & Chang, C. C. (2015). "A Framework for Dimensional and Surface Quality Assessment of Precast Concrete Elements Using BIM and 3D Laser Scanning." *Automation in Construction*, 49, 225-238.

Kim, M. K., Sohn, H., & Chang, C. C. (2014). "Automated Dimensional Quality Assessment of Precast Concrete Panels Using Terrestrial Laser Scanning." *Automation in Construction*, 45, 163-177.

Alzraiee, H., Sprotte, R., & Ruiz, A. L. (2020). "Quality Control for Concrete Steel Embed Plates using LiDAR and Point Cloud Mapping." *In ISARC. Proceedings of the International Symposium on Automation and Robotics in Construction*, 37, 727-734.

Enshassi, M. S., Walbridge, S., West, J. S., & Haas, C. T. (2020). "Dynamic and Proactive Risk-Based Methodology for Managing Excessive Geometric Variability Issues in Modular Construction Projects using Bayesian Theory." *Journal of Construction Engineering and Management*, 146(2), 04019096.